Integrative Biology

Accepted Manuscript

ROYAL SOCIETY OF CHEMISTRY

www.rsc.org/ibiology

High-throughput *in vivo* screening of biologics and delivery vehicles is achieved by automated delivery into target tissues of small vertebrates with developed organs. Individual zebrafish larvae are automatically oriented and immobilized within hydrogel droplets in an array format using a microfluidic system, and biologics are automatically microinjected to target organs with nearly perfect repeatability and precision.

High-throughput *in vivo* screening of biologics is achieved by automated delivery into target tissues of small vertebrates oriented and immobilized within arrays of hydrogel droplets.

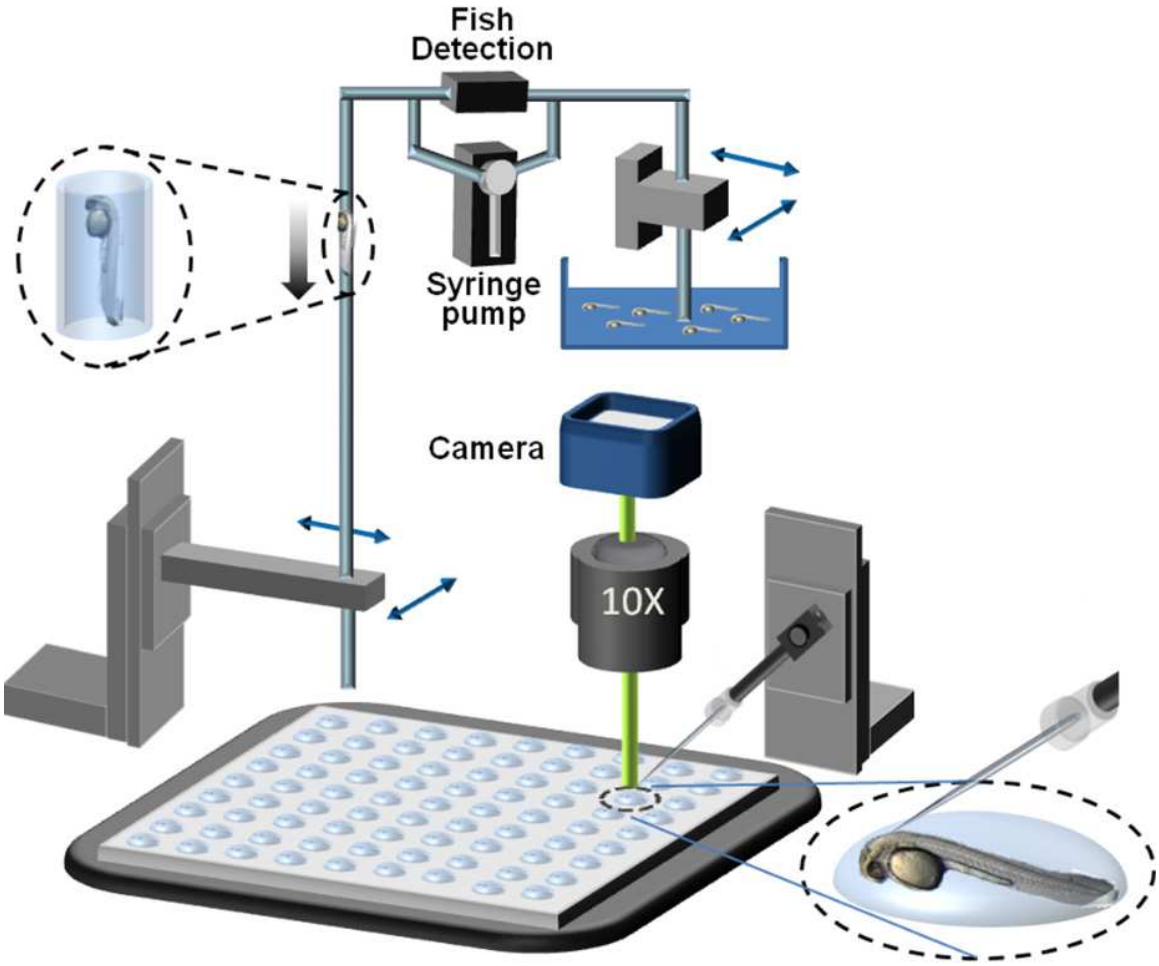

Organ-targeted high-throughput *in vivo* biologics screen identifies materials for RNA delivery

Tsung-Yao Chang[1], Peng Shi[1,2*], Joseph D. Steinmeyer[1], Itthi Chatnuntawech[1], Paul Tillberg[1], Kevin T. Love[3], Peter M. Eimon[1], Daniel G. Anderson[3], Mehmet Fatih Yanik[1,4*]

[1]Department of Electrical Engineering and Computer Science, Massachusetts Institute of Technology, Cambridge, Massachusetts, USA. [2]Department of Mechanical and Biomedical Engineering, City University of Hong Kong, Hong Kong, China. [3]Department of Chemical Engineering, Institute of Medical Engineering and Science, Division of Health Science and Technology, David H. Koch Institute for Integrative Cancer Research, Massachusetts Institute of Technology, Cambridge, Massachusetts, USA. [4]ETH, Zurich, Switzerland

[*]Correspondence should be addressed to

Dr. Peng Shi, pengshi@cityu.edu.hk

Dr. Mehmet Fatih Yanik, yanik@mit.edu

Keywords: high-throughput screening, microinjection, zebrafish larva, biologics, drug delivery vehicles, lipidoid materials

Abstract

Therapies based on biologics involving delivery of proteins, DNA, and RNA are currently among the most promising approaches. However, although large combinatorial libraries of biologics and delivery vehicles can be readily synthesized, there are currently no means to rapidly characterize them *in vivo* using animal models. Here, we demonstrate high-throughput *in vivo* screening of biologics and delivery vehicles by automated delivery into target tissues of small vertebrates with developed organs. Individual zebrafish larvae are automatically oriented and immobilized within hydrogel droplets in an array format using a microfluidic system, and delivery vehicles are automatically microinjected to target organs with nearly perfect repeatability and precision. We screened a library of lipid-like delivery vehicles for their ability to facilitate the expression of protein-encoding RNAs in the central nervous system. We discovered delivery vehicles that are effective in both larval zebrafish and rats. Our results showed that the *in vivo* zebrafish model can be significantly more predictive of both false positives and false negatives in mammals than *in vitro* mammalian cell culture assays. Our screening results also suggest certain structure-activity relationship, which can potentially be applied to design novel delivery vehicles.

Introduction

Biologics such as nucleic acids[1,2], proteins[3], cells[4], and nanoparticle vehicles for drug delivery[5] are currently under active investigation as therapeutics for a wide variety of human diseases. In contrast to chemically synthesized small molecules with enhanced solubility and permeability, these molecules have structures that are generally much larger and far more complex, and therefore require sophisticated modes of delivery[6-9]. Consequently, although large libraries of biologics and delivery vehicles are currently available[10-13], it remains challenging to rapidly assess their *in vivo* properties such as delivery efficiency, biodistribution, pharmacokinetics, tissue specificity, efficacy, and toxicity.

Zebrafish (*Danio rerio*) are being increasingly used for large-scale *in vivo* chemical and genetic screens. A combination of features, including small size, optical transparency, and rapid organogenesis, make zebrafish a vertebrate model that is uniquely suited for high-throughput screening (HTS)[14-16], which is cost-prohibitive in mammals. HTS of small molecules in zebrafish not only enables detection of adverse toxicity and off-target side effects in the early stages of pharmaceutical development[17], but has also led to the discovery of novel therapeutics currently undergoing clinical trials[18]. However, most biologics cannot be absorbed from the water due to their high molecular weight or unfavorable physical and chemical properties, and delivery of biologics into animals often requires manual microinjection[19], a process that is too slow and labor-intensive for HTS. Although automated microinjection systems have been developed for delivery of nucleic acids into the large yolk cells of zebrafish embryos immediately after fertilization[20], there is currently no high-throughput technology suitable for targeting specific organs of developed larvae and screening biologics *in vivo*, due to various technical challenges in different aspects of handling live larval zebrafish, including requirement of proper immobilization and orientation of larvae for micropipette to access different organs; difficulty to identify specific anatomic structures over transparent background; and lack of methods for parallel processing of

multiple larvae. Thus, although zebrafish is an established model for study of human disease and also function of organs such as CNS, liver, kidney, and even blood brain barrier which are all relevant to delivery and processing of biologics, no study of biologics or delivery vehicle formulations have been reported using zebrafish.

To address this need, we have developed an automated system for efficient delivery of biologics into target organs of zebrafish larvae for high-throughput *in vivo* screening. The system utilizes a microfluidic component to automatically distribute zebrafish larvae into an array of hydrogel droplets, each containing a single larva. While the hydrogel is still in a liquid state, vibrational stimulation or mild anesthesia is used to induce the larvae to assume either a dorsal or a lateral orientation. Subsequently, the substrate temperature is lowered causing the droplets to solidify and restrict all further motion. Next, the microinjection needle is automatically targeted to organs of interest using an image template-matching algorithm, and biologics are injected via a pressure driven system. Phenotypic outcomes, including *in vivo* distribution of biologics and gene expression, are then examined by optical imaging. Using this system, we screened a library of lipid-like compounds for their ability to facilitate the delivery and expression of oligonucleotides (protein-encoding RNAs) in the central nervous system (CNS) following injection into the cerebrospinal fluid (CSF) of the brain ventricles. Injection of biologics into CSF for therapeutics has been already used in clinical trials in neurodegenerative diseases[21]. Our screen discovered novel lipidoid formulations that facilitate efficient delivery of long RNA into CNS. We further showed that lipidoid activity in live rats is far better predicted by the *in vivo* zebrafish model than by a standard *in vitro* mammalian neural cell culture assay.

Results

High-throughput *in vivo* biologics delivery and screening

We developed an automated microinjection system for high-throughput delivery of biologics to target tissues of zebrafish larvae at 4 days post fertilization, a stage at which all major organs have formed (**Fig. 1**). Initially, zebrafish larvae are placed in a heated plate containing

embryo medium supplemented with 1% ultra-low gelling temperature agarose. The agarose-based hydrogel remains in the liquid phase at room temperature (25°C) and solidifies when briefly lowered below 17°C and increased back to 25°C. Brief exposure to this temperature range does not affect health of larvae[22], as we also verify below in assessment of our overall procedure's effect on health. Zebrafish larva are acquired from the reservoir using a microfluidic component we developed, which incorporates a multi-color multi-angle light-scattering and photo-detection system to discriminate individual larvae from debris and bubbles and to guarantee successful acquisition of a single larva[23, 24]**.** Next, a hydrogel droplet containing the larva is deposited onto a flat plate using a computer controlled syringe pump and motorized X-Y stage (**Movie S1**). The plate surface is pre-patterned with arrays of hydrophilic spots (96- or 48-well plate format) on a hydrophobic background, such that each hydrogel droplet remains confined within a precisely defined X-Y location in order to prevent mix-up with neighboring droplets. The use of hydrophilic spots surrounded by hydrophobic background allows generation of densely packed isolated droplets. We use droplet volumes large enough to avoid drying out, narrow enough to fit the array dimensions, and shallow enough to minimize the height of each hydrogel droplet to avoid optical distortion (25 μL for 96-spot arrays and 70 μL for 48-spot arrays).

The plate with arrays of larvae in liquid hydrogel droplets is transferred to a motorized X-Y stage with a thermoelectrically temperature-controlled substrate. To image and microinject to different organs of zebrafish, the larvae are manipulated to adopt one of two major orientations. For injection into dorsal targets, larvae within the hydrogel are agitated with several pulses of mechanical vibrations, which trigger a startle response that causes them to assume a dorsal-up orientation. For injection into lateral and ventral targets, larvae are anesthetized by addition of 0.2 mg/mL tricaine to the hydrogel solution, causing most to settle into a lateral orientation. After being properly oriented, the hydrogel droplets are solidified by cooling to 4°C with a thermoelectric module, which results in effective immobilization of the larvae within droplets. For larvae at 4 days post-fertilization (dpf), the success rates for dorsal and lateral orientation are

93±7% and 84±3%, respectively (**Table 1**, n = 323). With these methods, different organs within a larva, including forebrain, midbrain, ventricles, eyes, heart and liver, can be successfully targeted for microinjection (**Fig. 1b**).

Using an in-house developed image recognition program (see **Methods**) and a high-speed camera, the system automatically locates each larva within a hydrogel-droplet, positions the larvae to the center of field of view, and zooms in with motorized z-focus (**Fig. 1a, Movie S2**). Our algorithm identifies the eyes and the anterior-posterior axis of a larva, which can then be used as a reference coordinate to calculate the location of specific organs of interest. At the beginning of the microinjection process, the micropipette is front-loaded with biologics from a multiwell plate and then lowered to approach the target tissue/organ surface. By comparing of real-time the image of the larva's exterior surface with the one from previous sampling point while the micropipette approaches the target organ, our algorithms detect the distortion of the exterior surface by the needle prior to the needle's penetration into the larva. This allows our system to automatically not only identify the physical contact of the micropipette with the surface of the larva but also calculate its depth of penetration into the larva (see **Methods, Movie S3**). Subsequently, a pressure-driven picoliter-precision injector is triggered to deliver the biologics. The overall success rate of the automated microinjection into larval brain is 97% (n = 150). While the successful injection rate for other organs could be lower due to different properties, such as size, location, and movement etc., the hardware and algorithms could be further tuned according to specific applications. The average deviation of the automatically-targeted injection site from the desired site of injection (as determined by the user) is only 49 ± 3 μm (distance ± s.d., n = 75 from 3 separate experiments), allowing highly precise targeted delivery into specific organs. After microinjection, a self-adhesive bottomless multiwell chamber is attached onto the plate with arrays of larvae to isolate the hydrogel droplets from each other prior to a flushing process. The single-larva-containing hydrogel droplet in each well is then flushed with embryo medium to release the larvae from the droplets. It takes 20.0 ± 0.9 seconds per larva on average to finish a

complete cycle of loading, arraying, orientation, immobilization, target identification, microinjection, and recovery. This time can be further decreased to 13.1 ± 0.5 seconds per larva by pipelining the steps of arraying and injection (**Table 2**). This is considerably faster especially when compared to manual injection, which at least takes a trained technician several minutes[19, 25] to perform all the necessary procedures including anesthesia, immobilization, orientation of a single larva, and injection to the target organ. This is also exceptionally fast in practice, as one can screen thousands of delivery vehicle formulations/biologics in one week alone, which would otherwise take months to years if performed manually.

To evaluate whether the health of zebrafish larvae is affected by our system, we assessed 291 larvae using functional and morphological criteria (4 dpf) after passage through our system. Assessment of both survival and morphological abnormality (see methods) showed that our system caused no statistically significant adverse effects on zebrafish larvae with respect to controls (**Fig. 2**).

***In vivo* screening of lipidoids**

Using our automated organ-targeted delivery system, we screened a combinatorial library of lipid-like compounds termed 'lipidoids' to identify vehicles capable of facilitating efficient *in vivo* delivery of biologics into CNS tissues. This lipidoid library was synthesized using epoxide conjugation and is composed of amino alcohols consisting of polar amine-containing head groups and nonpolar hydrocarbon tails (lipidoids)[6]. We tested the entire library for *in vivo* delivery of protein-encoding RNAs to cells of the brain ventricle zone following injection into the CSF of the ventricular cavity. Delivery of biologics into CSF has particular translational value as similar approaches have been already employed in clinical trials for therapeutics of neurodegenerative diseases[21]. In contrast to DNA-based gene therapy, RNA offers an alternative strategy for the administration of therapeutic proteins without the risk of cell transformation[26, 27]. However, successful *in vivo* delivery of protein-coding RNAs has been a significant challenge due to their large size and susceptibility to enzymatic degradation[7, 27, 28].

In order to quantify RNA delivery efficiency, lipidoids were complexed with RNA (25 pg) encoding the fluorescent reporter protein mCherry. RNA:lipidoid complexes were formulated at a 1:10 weight-to-weight ratio and microinjected into the brain ventricles of zebrafish larvae using our system. Expression of mCherry was examined 24 hours post-injection by fluorescence imaging. Expression levels in the brain tissue were quantified by measuring the total mCherry fluorescence in each larva (n=10 per lipidoid). Our screen identified several lipidoids (such as C16-62) that significantly enhance *in vivo* delivery and expression of mCherry RNA in the CNS, and were far better than the tested commercially available products (**Fig. 3**).

Zebrafish are more predictive than cell culture of performance in rodents

To assess whether our screening results in zebrafish are predictive of outcomes in mammalian models, we selected the three most effective lipidoids (C16-62, C16-120, C12-120), and two low-scoring ones (C8-100 and C10-62) and tested them *in vivo* in rats. We injected mCherry RNA (0.1 μg) complexed with selected lipidoids into the lateral ventricles of adult rats using a stereotactic apparatus. Animals were allowed to recover for 48 hours before they were sacrificed, and brain tissue slices were collected. The expression levels of mCherry in the slices were quantified using the overall fluorescence within 250 μm of the ventricle wall, a distance comparable in size to the zebrafish brain (**Fig. 4a**). We also investigated the ability of an *in vitro* model to predict delivery efficiencies of these lipidoids in rodents by testing the same group of lipidoids in rat primary hippocampal cultures. 48 hours after seeding the cells, cultures were incubated in growth medium containing mCherry RNA complexed with lipidoids and then imaged to quantify the overall mCherry expression.

Interestingly, all lipidoids showed highly similar trends of *in vivo* RNA delivery efficiencies when tested in zebrafish or rodent animals. In both models, expression of mCherry was significantly increased above baseline in the presence of C16-62, C16-120, and C12-120, but not C8-100 or C10-62 (**Fig. 4b**). The active lipidoids showed clear differences in performance, with C16-62 performing significantly better than C12-120 in both *in vivo* models ($p < 0.05$ for

zebrafish, and $p < 0.01$ for rat). These trends were observed by both dot-blotting of mCherry protein from isolated tissue (**Fig. 4b**) and quantitative fluorescence imaging of brain slices (**Fig. 4c**). The overall correlation in delivery efficiencies of the lipidoids tested in zebrafish and rodent animals was very high, with a Pearson product-moment correlation coefficient of 0.97 (**Fig. 4d**). In contrast, the *in vitro* primary hippocampal culture model failed to identify C16-62, the most effective lipidoid in both rats and zebrafish ($p > 0.18$, **Fig. 4c**), and C16-120 was incorrectly predicted to be significantly more efficient than C16-62 ($p < 0.02$) by *in vitro* assay, although these compounds were not statistically different in either zebrafish or rodents ($p > 0.3$ for zebrafish, and $p > 0.1$ for rodents). In general, unlike the zebrafish model, the *in vitro* cell culture assay failed to show any strong correlation with the *in vivo* results in rodents (correlation coefficient = 0.47, **Fig. 4d**).

Discussion and Conclusion

Technologies for synthesizing biologics and specialized delivery vehicles have become increasingly sophisticated. However, large-scale assessment of their *in vivo* efficacy has remained challenging due to the lack of vertebrate animal models amenable to HTS. To address this significant need, we have developed an automatic organ-targeted microinjection system for screening biologics using zebrafish larvae. The system is based on a novel "fish-array" design, which creates arrays of hydrogel droplets, each containing a single larva, for delivery of biologics. We have demonstrated the capability of our system by screening a library of lipidoid compounds for their ability to efficiently deliver protein-coding RNAs into CNS cells following microinjection into the CSF.

Expression of specific proteins within the brain by delivery of encoding nucleic acids is potentially of great therapeutic value for a variety of CNS diseases[29]. Efficient RNA delivery is of particular interest for clinical applications where transient protein expression is desirable. For example, expression of neurotrophic proteins has the potential to provide both pre-operative

neuroportection[30] and to serve as an effective therapy following CNS or spinal cord injury. Trans-differentiation of reactive astrocytes to neuronal progenitors by delivery of transcription factor mRNAs expressing Sox2 or GATA3 may be another route for CNS regeneration following trauma or degeneration[31-33]. The use of RNA offers significant advantages over DNA-based gene therapy approaches, which present a number of safety concerns[27]. The clinical utility of therapeutic RNAs has so far been limited due to the strong immunogenicity, limited stability, and difficult delivery of RNAs *in vivo*. In recent years, we and others have shown that the immunogenicity of exogenous RNA can be suppressed by transiently and locally silencing the innate immune response[27, 34, 35]. However, *in vivo* delivery of RNA to most tissues still remains an unsolved challenge. The technology we have developed makes it possible for the first time to rapidly test numerous vehicle formulations for their ability to deliver RNA *in vivo*. The delivery scheme we used (i.e. injection of lipidoid-RNA complexes into CSF) is of direct clinical relevance, as lumbar intrathecal injection is anticipated to be a minimally invasive means for nonviral delivery to the CNS, and biologics delivered to the CSF has been shown to diffuse and distribute throughout extended regions of CNS in both rodents and humans[29, 36]. Our discovery of several vehicle formulations (C16-62, C16-120, C12-120) that are highly efficacious in rodent models without false positives suggest that zebrafish can be used as a model for high-throughput screening of biologics *in vivo* and, is more accurate than *in vitro* cell culture models in predicting outcomes in mammals. Interestingly, further analysis of our screening results also suggests certain structure-activity relationship, which can potentially be applied to design novel lipidoid delivery vehicles. The lipidoids are synthesized by conjugating amine-containing head groups and hydrocarbon tails[6, 11]. We found the length of hydrocarbon tails to be critical for the lipidoid's RNA carrier/delivery capability in CNS. No compounds with hydrocarbon tails less than 12 carbons were effective, which is in line with a previous report by Love *et al*[11]. For the amine head groups, amine 120 and 62 were in the top three most effective compounds (**Fig. 3a**). However, not all compounds based on amine 120 or 62 showed enhanced RNA delivery, such as C10-62

and C10-120, both of which showed very little efficacy in our *in vivo* screen, further suggesting the importance of proper length of non-polar chains.

The reliability of the system depends on successful implementation of all operational procedures, including fish loading, immobilization/orientation, and microinjection. For example, we reported a success rate of ~93% or ~97% for dorsal orientation and ventricle injection, respectively. Given an almost 100% loading reliability, our system can perform brain injection with ~90% reliability. It can potentially be used to automate and scale-up a variety of *in vivo* assays. For instance, zebrafish larvae have been shown to be a promising model for studying the blood-brain barrier and intravenous injection using our platform could be used to screen for vehicles that facilitate delivery of biologics from the circulatory system to the CNS. In addition, a number of disease models require precise delivery of cells to specific organs or body cavities. For example, human tumor cells have been injected into zebrafish to generate xenograft tumor models[37] and bacteria have been injected to model infection and pathogenesis[38]. Using manual microinjection to generate sufficient numbers of animals for large-scale chemical screens would be too laborious. Our system can be used for rapid implantation of cells on a scale that is compatible with HTS of chemical libraries to identify anti-tumorigenic or anti-infectious drug leads.

Methods and Materials

Surface treatment for generating fish-arrays. Transparent hydrophobic polystyrene plates were plasma-treated with the protection of a PDMS mask containing arrays of holes (48- or 96-well format) to create circular hydrophilic spots over a hydrophobic background. The diameters of the 48- and 96-well spots are 8 mm and 5 mm, respectively.

Image processing for automated microinjection. A coordinate system is established using the centroids of the both eyes, the swim bladder, and the axis of the trunk as landmarks. The eyes and swim bladder are identified based on their contrast with other larval surface features using a

threshold-based segmentation algorithm. An image of the larva embedded in agarose is first captured by a high-speed CCD camera (GX-1050, Prosilica) through a Nikon AZ-100 Multizoom microscope and then converted to a binary image using a threshold, where the threshold value is determined via statistical analysis of the overall illumination level of the image. Next, the objects in the binary image are filtered to eliminate smaller high-contrast objects such as melanocytes, leaving only the eyes and swim bladder. The filtering is performed by removing pixel-connected objects composed of pixels less than a threshold value. The threshold size is automatically adjusted to obtain only 3 objects from the images. Since the eyes are located closer to each other than they are to the swim bladder, the two objects with the least distance between their centroids are designated as eyes and the remaining object is recognized as the swim bladder. The anterior-posterior axis can be determined either by using curve-fitting along the centroids of eyes and swim bladder or by rotation image-correlation with a reference image of larva. Automated injection is then performed by diagonally lowering the injection micropipette (Micromanipulator: Patchman NP2, Eppendorf; Injector: Xenoworks, Sutter Instrument) to approach the target while monitoring the difference between real-time images and the pre-injection images to detect the contact and penetration of the micropipette tip. Specifically, after the micropipette tip contacts the exterior of the larva, but before it actually penetrates any tissue, the difference between the real-time images and the pre-injection images increases dramatically as the tissue is pressed by the tip and deforms. Following the penetration of the micropipette into the tissue, the image difference decreases as the tissue deformation relaxes. After penetration is detected, a 1 nL volume is injected by triggering a pressure drive picoliter microinjector (Sutter Instrument). Following injection, the micropipette is retracted to the home position. The automation control of microinjector and data readout is through NIDAQ cards (NI 9422; NI USB-6211). Software is developed on Matlab and can be provided by request.

Health assessment of larvae processed by the system. For health assessment and all subsequent experiments, the syringe pump was operated at aspiration rates of 330 μL/s. 4 dpf larvae were

loaded from a reservoir, deposited onto the surface-treated plate, microinjected with 1 nL of PBS, and recovered for assessment by briefly flushing the surface of each hydrogel droplet with low-pressure stream of embryo medium. In total, 291 larvae were processed and compared with a control group of 187 larvae from the same clutch. Health assessment was based on both functional and morphological criteria. Functional criteria included visual confirmation of normal heartbeat and reflex response to touch stimuli. Morphological criteria included spine bending (i.e. lordosis, kyphosis, and scoliosis) and craniofacial abnormalities[39]. Larvae were assessed immediately after recovery from the hydrogel droplets and again every 24 hours over the course of the next 4 days.

RNA synthesis. Templates for *in vitro* transcription were prepared as previously reported[34]. Briefly, the mCherry open reading frame, flanked by the human β-globin (HBB) 5′- and 3′-untranslated regions (UTRs), was cloned into the pCR-Blunt II-TOPO vector (Invitrogen). A strong Kozak consensus sequence was included between the 5′-UTR and the protein-coding sequence to promote efficient translation of the encoded protein. Templates were amplified using high-fidelity PCR (Kapa Biosystems) and *in vitro* synthesis of Cap 1-capped polyadenylated RNA was carried out using the mScript mRNA Production System (CELLSCRIPT, Inc.). Pseudouridine and 5-methylcytidine were substituted for uridine and cytidine in all *in vitro* transcribed RNAs. RNAs were purified using RNeasy Midi Kits (Qiagen) and the quality of the transcripts was assessed by denaturing agarose gel electrophoresis.

Lipidoid-RNA formulations. The lipidoids were dissolved in ethanol to make 50 mg/mL stock solutions. The stock solutions were sonicated for 5 minutes immediately before being diluted in PBS to 5 mg/mL. To formulate lipidoid-RNA complexes, 0.5 μg of mCherry RNA was mixed with lipidoids in PBS at a 1:10 weight ratio to make 20 μL working solutions. The lipidoid-RNA mixture was incubated for 15 minutes at room temperature prior to injection into animals or addition to cell culture medium.

Stereotactic injection to rats. Sprague-Dawley rats (<350 g) were purchased from Charles River Laboratory. Young adult female rats were dosed with buprenorphine and meloxicam two hours prior to isoflurane-based anesthesia administration. The scalp was opened and retracted. An entry hole (~3 mm in diameter) for injections was made through the skull using a dental drill with burr bit. Injections were made into the lateral ventricle at stereotactic coordinates -3.0 RC -0.5 ML -15 DV mm using 10 μL Hamilton syringes. 4 μL of mCherry RNA-lipidoid complex was injected at a rate of 0.06 μL/s. Following injection, the skull was cemented and the scalp was sutured. Animals were given post-operative dosages of buprenorphine and meloxicam at 8 hours following surgery and every 12 hours thereafter. 48 hours after injection, animals were sacrificed and brain tissue was immediately collected. 200 μm thick whole brain coronal slices were taken using a Vibratome (Leica), and either fixed and stained or immediately imaged. All animal work was carried out with prior approval of MIT's Committee on Animal Care (CAC) and the Department of Comparative Medicine (DCM) and was in accordance with local, state, and federal animal care guidelines.

Dot blotting of rat brain tissues. A total 200 μg of tissue along the ventricle wall was dissected from each animal and kept frozen. Proteins were extracted from the tissues using a total protein extraction kit (Millipore). The proteins were analyzed through standard blotting procedures to semi-quantitatively confirm the expression of mCherry in the brain ventricle region.

Assessment of *in vitro* delivery efficacy using primary rat primary hippocampal cultures. Primary cells were harvested from the hippocampi of E18 Sprague-Dawley rat pups obtained from Charles River Laboratories. Hippocampal tissue was digested using papain and mechanical trituration. Cells were plated onto poly-ornithine/laminin coated 24-well plates with a density of approximately 100,000 per well. Cells were cultured in medium composed of 50/50 DMEM/F12, 0.5× N2 and 0.5× B27 supplements. 1% Penicillin/Streptomycin was added to the medium for the first 36 hours following harvest and subsequently removed 4 hours before transfection to avoid adverse effects on lipid-based delivery vehicles. Transfections were carried out by adding 20 μL

of the lipidoid-RNA complex (containing a total of 0.5 μg RNA) to each well and incubating the primary hippocampal cultures at 37°C for 24 hours. After incubation, mCherry expression was observed via fluorescence imaging with 10X magnification, and the images were analyzed using Nikon Elements AR.

Acknowledgements

All zebrafish used in these studies were raised and maintained in the Koch Institute Zebrafish Core Facility directed by Dr. Nancy Hopkins. We thank Dr. Adam Amsterdam for his oversight of the fish facility and Tim Angellini for technical assistance in raising and maintaining the fish. We thank the following funding sources: NIH Transformative Research Award (R01 NS073127), NIH Director's Innovator award (DP2 OD002989), Packard award in Science and Engineering, Sanofi Pharmaceuticals, Foxconn Sponsorship and Hertz fellowship. P.S. is also supported by an early career award from UGC Hong Kong (125012), NSFC (81201164), ITC (ITS/376/13) and grants from City University of Hong Kong (9610215, 7200269).

Author contributions

T.-Y.C., P.S., and M.F.Y. conceived the project, designed the experiments and wrote the manuscript. P.M.E. contributed in writing the manuscript. T.-Y.C., P.S., J.D.S., P.T. and I.C. performed the experiments. K.L., D.A. and R.L. synthesized and provided the lipidoid material library and commented the manuscript.

References

1. J. C. Burnett and J. J. Rossi, *Chemistry & biology*, 2012, 19, 60-71.
2. A. S. Harms, C. J. Barnum, K. A. Ruhn, S. Varghese, I. Trevino, A. Blesch and M. G. Tansey, *Molecular therapy : the journal of the American Society of Gene Therapy*, 2011, 19, 46-52.
3. W. Stohl and D. M. Hilbert, *Nature biotechnology*, 2012, 30, 69-77.
4. S. U. Kim and J. de Vellis, *Journal of neuroscience research*, 2009, 87, 2183-2200.
5. F. Alexis, E. M. Pridgen, R. Langer and O. C. Farokhzad, *Handbook of experimental pharmacology*, 2010, 55-86.
6. A. Akinc, A. Zumbuehl, M. Goldberg, E. S. Leshchiner, V. Busini, N. Hossain, S. A. Bacallado, D. N. Nguyen, J. Fuller, R. Alvarez, A. Borodovsky, T. Borland, R. Constien, A. de Fougerolles, J. R. Dorkin, K. Narayanannair Jayaprakash, M. Jayaraman, M. John, V. Koteliansky, M. Manoharan, L. Nechev, J. Qin, T. Racie, D. Raitcheva, K. G. Rajeev, D. W. Sah, J. Soutschek, I. Toudjarska, H. P. Vornlocher, T. S. Zimmermann, R. Langer and D. G. Anderson, *Nature biotechnology*, 2008, 26, 561-569.
7. A. D. Judge, V. Sood, J. R. Shaw, D. Fang, K. McClintock and I. MacLachlan, *Nature biotechnology*, 2005, 23, 457-462.
8. D. B. Rozema, D. L. Lewis, D. H. Wakefield, S. C. Wong, J. J. Klein, P. L. Roesch, S. L. Bertin, T. W. Reppen, Q. Chu, A. V. Blokhin, J. E. Hagstrom and J. A. Wolff, *Proceedings of the National Academy of Sciences of the United States of America*, 2007, 104, 12982-12987.
9. T. S. Zimmermann, A. C. Lee, A. Akinc, B. Bramlage, D. Bumcrot, M. N. Fedoruk, J. Harborth, J. A. Heyes, L. B. Jeffs, M. John, A. D. Judge, K. Lam, K. McClintock, L. V. Nechev, L. R. Palmer, T. Racie, I. Rohl, S. Seiffert, S. Shanmugam, V. Sood, J. Soutschek, I. Toudjarska, A. J. Wheat, E. Yaworski, W. Zedalis, V. Koteliansky, M. Manoharan, H. P. Vornlocher and I. MacLachlan, *Nature*, 2006, 441, 111-114.
10. C. Falschlehner, S. Steinbrink, G. Erdmann and M. Boutros, *Biotechnology journal*, 2010, 5, 368-376.
11. K. T. Love, K. P. Mahon, C. G. Levins, K. A. Whitehead, W. Querbes, J. R. Dorkin, J. Qin, W. Cantley, L. L. Qin, T. Racie, M. Frank-Kamenetsky, K. N. Yip, R. Alvarez, D. W. Sah, A. de Fougerolles, K. Fitzgerald, V. Koteliansky, A. Akinc, R. Langer and D. G. Anderson, *Proceedings of the National Academy of Sciences of the United States of America*, 2010, 107, 1864-1869.
12. X. Yang, N. Li and D. G. Gorenstein, *Expert opinion on drug discovery*, 2011, 6, 75-87.
13. P. Shi, M. A. Scott, B. Ghosh, D. Wan, Z. Wissner-Gross, R. Mazitschek, S. J. Haggarty and M. F. Yanik, *Nat Commun*, 2011, 2, 510.
14. G. J. Lieschke and P. D. Currie, *Nature reviews. Genetics*, 2007, 8, 353-367.
15. C. Parng, W. L. Seng, C. Semino and P. McGrath, *Assay and drug development technologies*, 2002, 1, 41-48.
16. L. I. Zon and R. T. Peterson, *Nature reviews. Drug discovery*, 2005, 4, 35-44.
17. P. M. Eimon and A. L. Rubinstein, *Expert opinion on drug metabolism & toxicology*, 2009, 5, 393-401.
18. T. E. North, W. Goessling, C. R. Walkley, C. Lengerke, K. R. Kopani, A. M. Lord, G. J. Weber, T. V. Bowman, I. H. Jang, T. Grosser, G. A. Fitzgerald, G. Q. Daley, S. H. Orkin and L. I. Zon, *Nature*, 2007, 447, 1007-1011.
19. J. H. Gutzman and H. Sive, *Journal of visualized experiments : JoVE*, 2009.
20. W. Wang, X. Liu, D. Gelinas, B. Ciruna and Y. Sun, *PloS one*, 2007, 2, e862.

21. J. G. Nutt, K. J. Burchiel, C. L. Comella, J. Jankovic, A. E. Lang, E. R. Laws, Jr., A. M. Lozano, R. D. Penn, R. K. Simpson, Jr., M. Stacy and G. F. Wooten, *Neurology*, 2003, 60, 69-73.
22. Y. Long, G. Song, J. Yan, X. He, Q. Li and Z. Cui, *BMC Genomics*, 2013, 14, 612.
23. T. Y. Chang, C. Pardo-Martin, A. Allalou, C. Wahlby and M. F. Yanik, *Lab on a chip*, 2012, 12, 711-716.
24. C. Pardo-Martin, T. Y. Chang, B. K. Koo, C. L. Gilleland, S. C. Wasserman and M. F. Yanik, *Nature methods*, 2010, 7, 634-636.
25. J. L. Cocchiaro and J. F. Rawls, *Journal of visualized experiments : JoVE*, 2013, e4434.
26. G. F. Jirikowski, P. P. Sanna, D. Maciejewski-Lenoir and F. E. Bloom, *Science*, 1992, 255, 996-998.
27. M. S. Kormann, G. Hasenpusch, M. K. Aneja, G. Nica, A. W. Flemmer, S. Herber-Jonat, M. Huppmann, L. E. Mays, M. Illenyi, A. Schams, M. Griese, I. Bittmann, R. Handgretinger, D. Hartl, J. Rosenecker and C. Rudolph, *Nature biotechnology*, 2011, 29, 154-157.
28. J. M. Vargason, G. Szittya, J. Burgyan and T. M. Hall, *Cell*, 2003, 115, 799-811.
29. P. Leone, C. G. Janson, L. Bilaniuk, Z. Wang, F. Sorgi, L. Huang, R. Matalon, R. Kaul, Z. Zeng, A. Freese, S. W. McPhee, E. Mee and M. J. During, *Ann Neurol*, 2000, 48, 27-38.
30. Y. J. Cao, T. Shibata and N. G. Rainov, *Gene therapy*, 2002, 9, 415-419.
31. R. Blum, C. Heinrich, R. Sanchez, A. Lepier, E. D. Gundelfinger, B. Berninger and M. Gotz, *Cereb Cortex*, 2011, 21, 413-424.
32. C. Kizil, N. Kyritsis, S. Dudczig, V. Kroehne, D. Freudenreich, J. Kaslin and M. Brand, *Dev Cell*, 2012, 23, 1230-1237.
33. S. Robel, B. Berninger and M. Gotz, *Nat Rev Neurosci*, 2011, 12, 88-104.
34. M. Angel and M. F. Yanik, *PloS one*, 2010, 5, e11756.
35. K. Kariko, H. Muramatsu, F. A. Welsh, J. Ludwig, H. Kato, S. Akira and D. Weissman, *Molecular therapy : the journal of the American Society of Gene Therapy*, 2008, 16, 1833-1840.
36. D. M. Anderson, L. L. Hall, A. R. Ayyalapu, V. R. Irion, M. H. Nantz and J. G. Hecker, *Hum Gene Ther*, 2003, 14, 191-202.
37. A. M. Taylor and L. I. Zon, *Zebrafish*, 2009, 6, 339-346.
38. K. Takaki, C. L. Cosma, M. A. Troll and L. Ramakrishnan, *Cell Rep*, 2012, 2, 175-184.
39. S. R. Blechinger, J. T. Warren, Jr., J. Y. Kuwada and P. H. Krone, *Environ Health Perspect*, 2002, 110, 1041-1046.

Figures and Legends

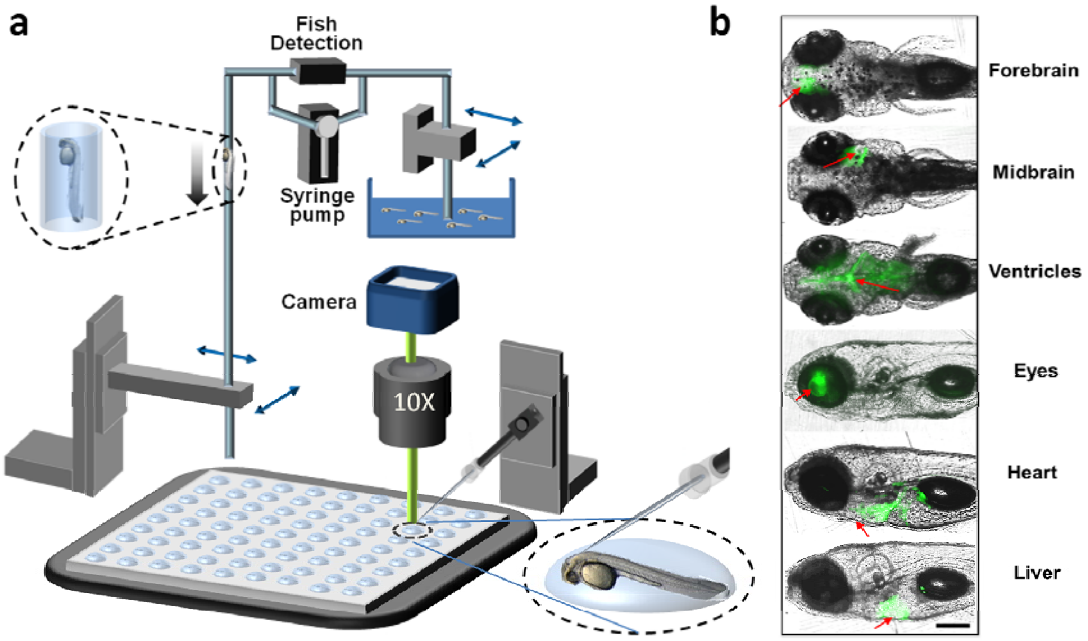

Figure 1. The fish-array based automatic organ-targeted microinjection system. (**a**) Setup of the system. Larvae in liquid phase of ultra-low gelling temperature agarose hydrogel are automatically loaded from a reservoir into the system with a microfluidic component, and arrayed onto a surface-treated plate as single-larva-containing hydrogel droplets. Both the loading reservoir and arraying plates are placed on motorized X-Y stages, and the loading and dispensing nozzles are mounted on motorized Z stages. Depending on the desired orientation, the larvae are either agitated with a vibrating motor attached to the plate (for dorsal-up orientation) or anesthetized prior to loading (for them to orient laterally). Larvae are immobilized by cooling with a thermoelectric cooler to rapidly solidify the hydrogel droplets. The system automatically identifies each larva, positions the targeted region under the injection micropipette, and detects the contact and penetration of the tip of the micropipette. A computer-controlled pressure driven microinjector is then triggered to inject test compounds into the target organ. After injection, a self-adhesive bottomless multiwell chamber is attached to the plate and the larvae are recovered from the hydrogel by gently flushing each droplet with embryo medium. (**b**) Images of zebrafish larvae following automatic microinjection of FITC-coupled dextran molecules into different organs using the system.

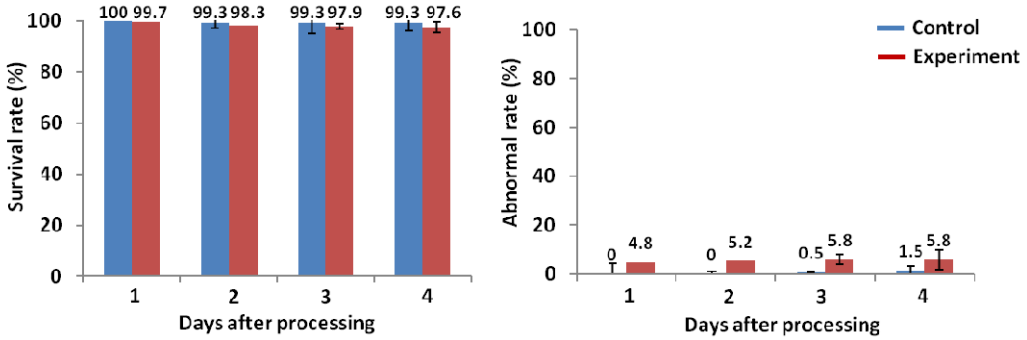

Figure 2. Health assessment of larvae after operations. (**a**) Survival rate of larvae following autonomous microinjection (red bars; n = 291) compared to control larvae from the same clutch (blue bars; n=187). (**b**) Percentage of larvae exhibiting morphological abnormalities following operations (red bars; n = 291) compared to control larvae from the same clutch (blue bars; n=187).

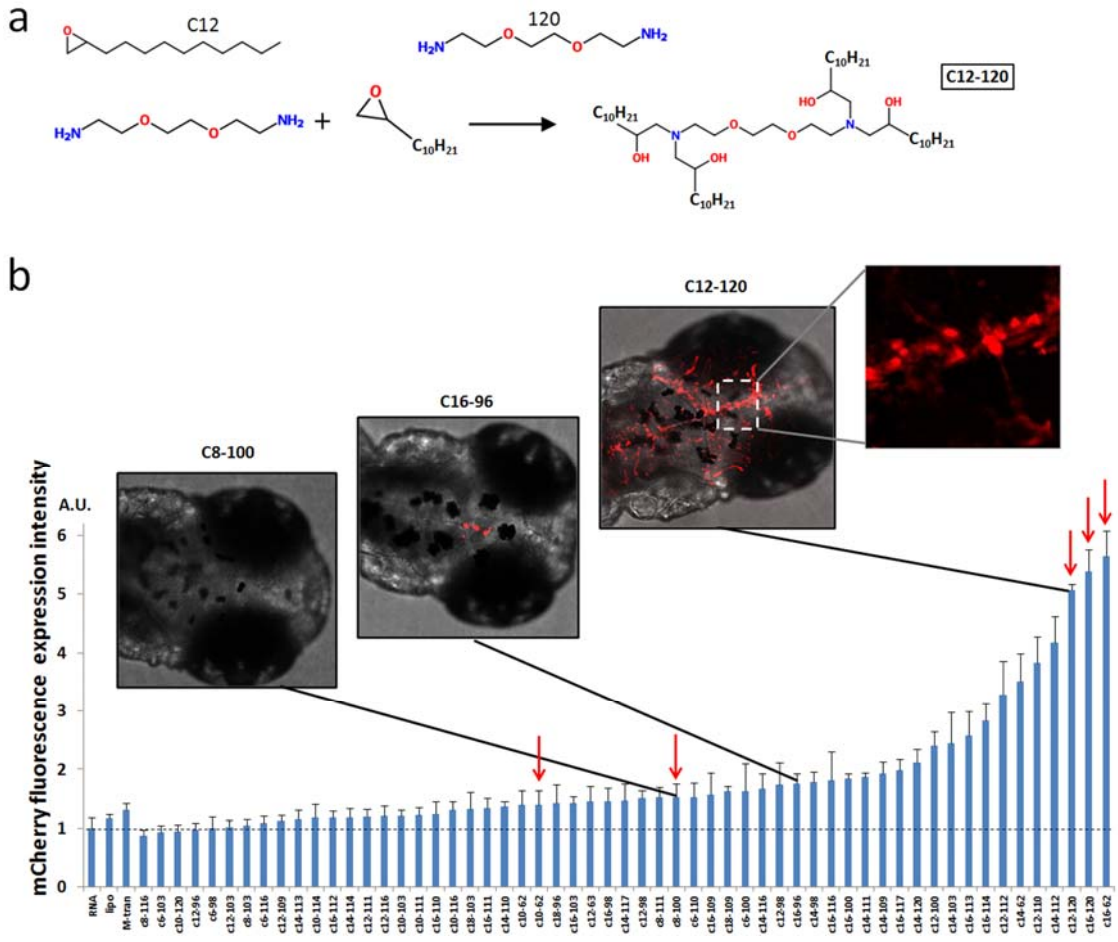

Figure 3. *In vivo* high-throughput screening of a lipidoid library in larval zebrafish. **a**) The structure of a sample lipidoid material. **b**) Screening of vehicles for delivering RNA into CNS. RNA encoding full-length mCherry fluorescent protein was complexed with lipidoids and microinjected into the brain ventricles of 4 dpf larvae (n = 10 larvae per lipidoid compound). Insets of fluorescence images show expression of mCherry in brain tissue of the larva. The *in vivo* RNA delivery efficiency of all lipidoids was determined by quantifying total mCherry fluorescence intensity within the brain region of each larva. Red arrows indicate lipidoid compounds that were selected for further tests in rodents and primary hippocampal cultures.

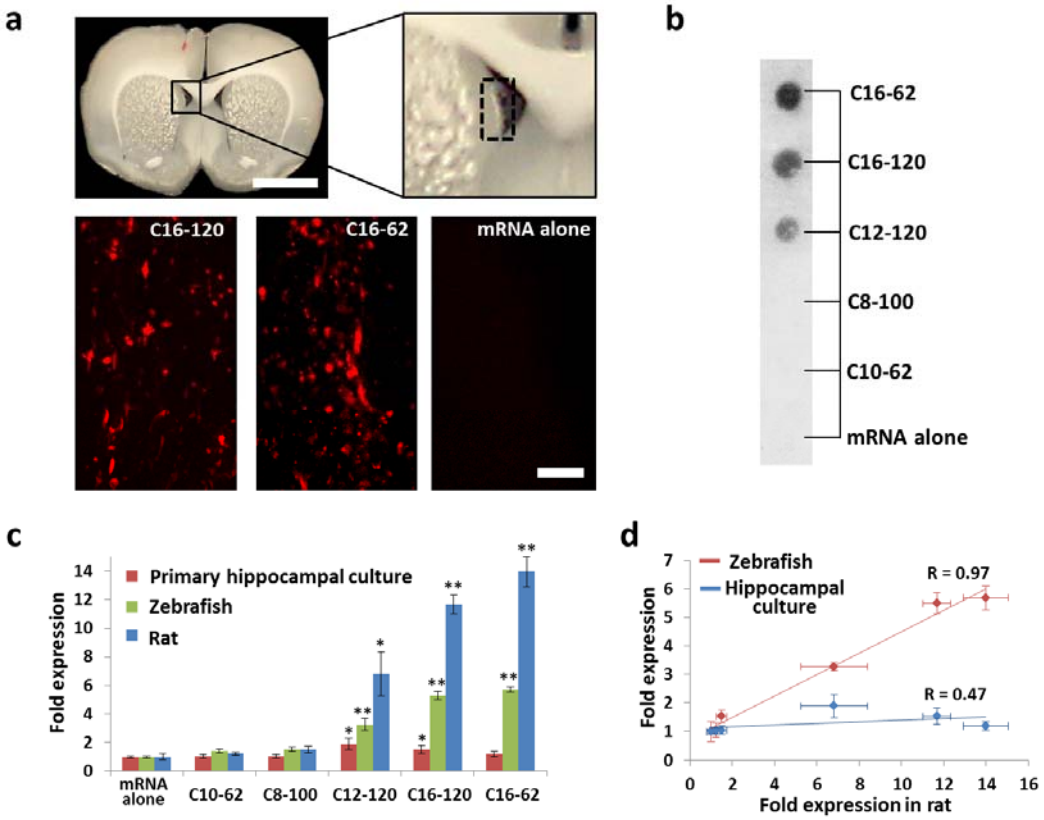

Figure 4. Comparison of lipidoid-mediated RNA transfection efficiencies in different models. (**a**) Images of a coronal rat brain slice near the injection site, scale bar = 5 mm. Lipidoids complexed with RNA were stereotaxically injected into the brain ventricles of adult SD rats. The black dashed box indicates the region used for quantification of mCherry protein expression. Fluorescence images show mCherry expression in the brain ventricle of rats injected with RNA alone, or with RNA complexed with lipidoid compounds, C16-120 and C16-62. Scale bars = 100 μm. (**b**) Image of Dot-blot showing mCherry protein expression levels in the rat brain tissues. (**c**) Quantification of lipidoid-mediated expression of mCherry in three different testing models, primary hippocampal cultures (red), zebrafish larvae (green) and rodent animal (blue), after delivering of lipidoid complexed RNA. Asterisks indicate significant differences with respect to RNA alone controls (* $p < 0.05$, ** $p < 0.01$; *t*-test, single-tailed). (**d**) Correlation between results from different testing models: rats *vs.* zebrafish (red), and rats *vs.* primary hippocampal culture (blue). The delivery efficiencies of tested lipidoid compounds from rodent models correlate well with the *in vivo* zebrafish model but not with results from *in vitro* primary hippocampal cultures. Expression levels in (**c**) and (**d**) are normalized with respect to control conditions.

Tables

Table 1. Performance of the orientation mechanisms.

Orientation mechanism	Success rate* (%)
Dorsal orientation by stimulation	93.4 ± 2.9
Lateral orientation by anesthetization	13.6 ± 6.6
Dorsal orientation without stimulation	60.0 ± 3.2

*n = 323

Table 2. Timeline of the autonomous microinjection operations.

Processing Step	**Time ± s.d.*** **(sec/larva)**
Loading and arraying	13.1 ± 0.5
Positioning	1.0 ± 0.2
Injecting	5.1 ± 0.1
Orientation and immobilization in 96-well format	0.8 ± 0.1
Overall duration for each larva in series	20.0 ± 0.9
Overall duration for each larva after pipelining	13.1 ± 0.5
Test samples front-loading	19.9 ± 6.9

*n = 60 for each